

# Molecular Recognition and Interaction between Uracil and Urea in Solid-State Studied by Terahertz Time-Domain Spectroscopy

Jingqi Yang,<sup>†,‡</sup> Shaoxian Li,<sup>†,‡</sup> Hongwei Zhao,<sup>\*,†</sup> Bo Song,<sup>†</sup> Guoxin Zhang,<sup>†</sup> Jianbing Zhang,<sup>†</sup> Yiming Zhu,<sup>§</sup> and Jianguang Han<sup>\*,†</sup>

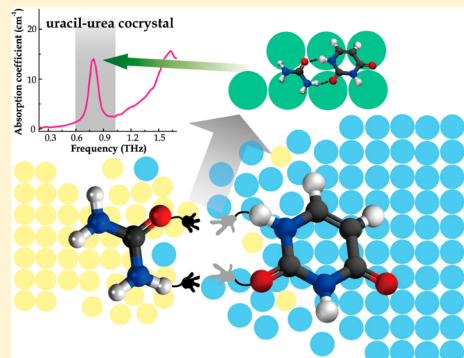
<sup>†</sup>Key Laboratory of Interfacial Physics and Technology, Shanghai Institute of Applied Physics, Chinese Academy of Sciences, Shanghai 201800, People's Republic of China

<sup>‡</sup>Center for Terahertz Waves and College of Precision Instrument and Optoelectronics Engineering, Tianjin University, Tianjin 300072, People's Republic of China

<sup>§</sup>Engineering Research Center of Optical Instrument and System, Ministry of Education, University of Shanghai for Science and Technology, Shanghai 200093, People's Republic of China

## S Supporting Information

**ABSTRACT:** Using terahertz time-domain spectroscopy characterization, we observe that urea is able to recognize and interact with uracil efficiently even in the solid phase without involving water or solvents. A cocrystal configuration linked by a pair of hydrogen bonds between uracil and urea was formed. The terahertz absorption spectrum of the cocrystal shows a distinct new absorption at 0.8 THz ( $26.7\text{ cm}^{-1}$ ), which originates from the intermolecular hydrogen bonding. Both mechanical milling and heating can accelerate the reaction efficiently. Density functional theory was adopted to simulate the vibrational modes of the cocrystal, and the results agree well with the experimental observation. Multiple techniques, including powder X-ray diffraction, scanning electron microscopy, and Fourier transform infrared spectroscopy, were performed to investigate the reaction process, and they presented supportive evidence. This work enables in-depth understanding of recognition and interaction of urea with nucleobases and comprehension of the denaturation related to RNA. We also demonstrate that terahertz spectroscopy is an effective and alternative tool for online measurement and quality control in pharmaceutical and chemical industries.



## 1. INTRODUCTION

The low frequency resonance absorption of molecules in the terahertz (THz) regime is drawing increasing attention recently. Terahertz resonance behavior of molecules, always originating from weak interaction, such as hydrogen bonding and van der Waals forces, and crystal lattice vibrations, plays important roles in the network structure, interactions, and functionality of biomolecules. A series of biomolecules, such as nucleic acid bases and amino acids, have been investigated by THz time-domain spectroscopy (THz-TDS), and the unique characteristic features were suggested to be potential probes for label-free detection of DNA and protein.<sup>1–3</sup> The high sensitivity of THz spectroscopy provides a particular fingerprint method to discriminate and identify molecules, such as different DNA sequences, hybridization states and perturbation by ligands.<sup>4–8</sup> Recently, the noncovalent interactions between nucleic acid base pairs in the cocrystal were investigated using THz spectroscopy by King et al., and the results indicated that the hydrogen bonding interaction is responsible for the molecular orientations.<sup>9,10</sup> The THz technique has been proven to be an important analytical approach in chemical and pharmaceutical analysis. It has the capability to distinguish

polymorphism of compounds and to monitor the cocrystallization process in solid state.<sup>11–13</sup>

Urea always serves as an effective denaturant for proteins and genetic materials. Plenty of work has been done to understand the denaturing effect of urea in the background of aqueous solution.<sup>14–17</sup> However, unlike the relatively well-understood action mechanism of urea on proteins, the underlying molecular mechanism of urea-induced denaturation of nucleic acids has not yet been explored. Urea, with both carbonyl and amino groups, can interact with biomolecules by donating or accepting hydrogen bonds. Molecular simulations by Yoon et al. revealed that the denaturation of RNA structures is mainly driven by hydrogen bonding and stacking interactions of urea with the bases.<sup>18</sup> The interaction of urea with nucleic acid functional groups has been quantified by Guinn et al. recently. Urea was suggested as a solute probe to characterize the conformational changes in nucleic acid processes. They found that the interactions of urea with heterocyclic aromatic rings

Received: June 18, 2014

Revised: October 27, 2014

Published: October 28, 2014

and attached methyl groups are particularly favorable relative to interactions with water.<sup>17</sup> A THz absorption spectroscopy study by the Havenith group has revealed the molecular behavior of urea in aqueous solution, where urea and water were readily interchangeable.<sup>19</sup> The results also supported a direct mechanism of denaturation by urea rather than the indirect mechanism that classifies urea as a structure breaker. Although there are still debates about the molecular mechanism and denaturing power of urea, the synergistic interaction between urea and water molecules is necessary and critical.<sup>20</sup> Interestingly, in our study, an evident interaction between urea and uracil was observed even in the solid state without the participation of water or solvent. The new emerging absorption from THz-TDS measurement directly demonstrates the occurrence of solid-state reaction. Our experiment implies that urea can induce gene material mutation even in a dry environment.

In this work, molecular recognition and interaction between uracil and urea in the solid state were investigated by use of THz-TDS. The obtained cocrystal product was also verified by powder X-ray diffraction (PXRD), scanning electron microscopy (SEM), and Fourier transform infrared spectroscopy (FTIR). The promoting effects of mechanical milling and heating were investigated. To rationalize the observed transformation in the experiment, an *ab initio* method based on density functional theory (DFT) was applied.

## 2. EXPERIMENTAL SECTION

**2.1. Material.** Urea ( $\geq 99\%$ ) and potassium bromide (KBr, 99%) were commercially available at Sinopharm Chemical Reagent Co., Ltd. Uracil (99%) and the polyethylene powder (particle size 53–75  $\mu\text{m}$ ) were obtained from Sigma-Aldrich. All chemicals were used without further purification.

**2.2. Sample Preparation.** The cocrystal of urea and uracil was obtained from solution. Equimolar amounts of uracil and urea were fully dissolved in water under ultrasonic treatment. The solution was then rotovapitated to complete dryness. White fine powder was obtained and then dried under low vacuum overnight.

The solid-state reaction was performed by cogrinding equimolar amounts of urea and uracil at room temperature, using a planetary ball mill (QM-3SP04, gear type, Nanjing University instrument plant). The rpm (revolutions per minute) was 500, and the ratio between large ball ( $\Phi 10\text{ mm}$ ) and small ball ( $\Phi 6\text{ mm}$ ) was 1:6. Both urea and uracil were pretreated by milling into fine particles to improve the uniformity and dispersity. A measured amount of product yielded in the solid-state reaction at different milling times was taken out for further analysis.

**2.3. THz-TDS.** The THz-TDS setup is a standard transmission-type TDS system based on photoconductive switches for generation and detection.<sup>21</sup> The whole system was placed in a closed box purged with dry nitrogen to keep the relative humidity less than 2.0%, and all the THz spectra were measured at room temperature. Powder sample (50 mg) and 150 mg of polyethylene were gently ground together using a mortar and pestle and then pressed into pellets (13 mm in diameter and  $1.62 \pm 0.05\text{ mm}$  in thickness) with an oil press at a pressure of 2 MPa. The tablet surfaces were kept smooth and parallel. Absorption coefficients of the tablets were extracted from their transmitted THz pulses. More details about the data analysis method are described elsewhere.<sup>22</sup>

**2.4. Temperature Enhanced Solid-State Reaction.** Equimolar urea and uracil powder (with pretreating) were mixed together, ground thoroughly, and pressed into a 0.9 mm thick pellet and placed into a heating chamber. The temperature was controlled with an accuracy of  $\pm 0.5\text{ }^\circ\text{C}$  using a variable temperature controller (Specac, UK) with a heating rate  $2.5\text{ }^\circ\text{C}/\text{min}$ . The temperature increased from 20 to  $120\text{ }^\circ\text{C}$  with an interval of  $10\text{ }^\circ\text{C}$ . Then the temperature was kept at  $120\text{ }^\circ\text{C}$  for about 60 min until the THz spectrum was no longer varying.

**2.5. SEM.** SEM photographs were recorded on gold-coated samples at room temperature, using a LEO 1530 VP SEM. The working distance (WD) was 4.3 mm, and the extra high tension (EHT) was 5.0 kV.

**2.6. PXRD.** The powder samples were loaded into a cavity of a glass sample holder then gently compacted with a glass slide to make a smooth and flat sample surface. PXRD was measured using an X'Pert Pro MPD (Cu source, 40 kV voltages, and 40 mA filament emission). The data were collected with a scan range from  $10^\circ$  to  $100^\circ$  ( $2\theta$ ), and  $10^\circ$  to  $40^\circ$  was chosen to have a clear view of the difference.

**2.7. FTIR.** FTIR spectra were recorded using a TENSOR27 FTIR spectrometer (Bruker Optics) at room temperature. Spectra were collected in the range of  $400\text{--}4000\text{ cm}^{-1}$  for 32 scans. Powder samples were manually mixed with dry KBr in an agate mortar and pressed into thin pellets.

## 3. RESULTS AND DISCUSSION

**3.1. THz Spectroscopy.** The THz absorption spectra of uracil and urea in the range of 0.2–2 THz are shown in Figure 1. Both present no obviously sharp peaks but slowly increasing absorption. When an equimolar amount of urea and uracil powder (without pretreating) were gently mixed together, no obvious absorption peak was observed. However, a new peak at 0.8 THz emerged after the samples were laid up for several days at room temperature, indicating some changes happened (Figure 1d). An identical peak was also observed in the

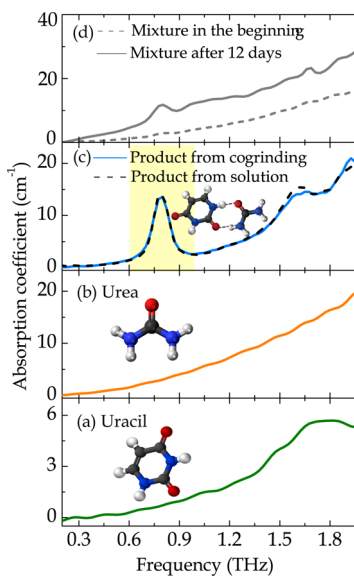


**Figure 1.** THz absorption spectra of (a) uracil, (b) urea, (c) uracil-urea product yielded from cogrinding and from aqueous solution, and (d) gently mixed uracil-urea mixtures in the beginning and 12 days later.

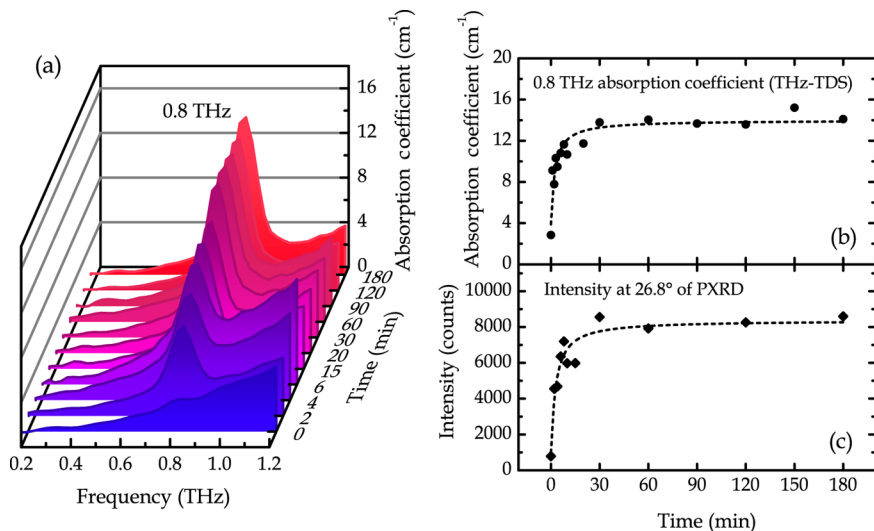


**Figure 2.** (a) THz absorption spectra of the reaction process of urea and uracil by cogrinding (0.2–1.2 THz range was taken for a clear view). (b) THz absorption intensity at 0.8 THz of the coground mixtures as a function of time. (c) Peak intensity at  $26.8^\circ$  of PXRD of the coground mixtures as a function of time. The dashed line in panels b and c is provided as a guide to the eye.

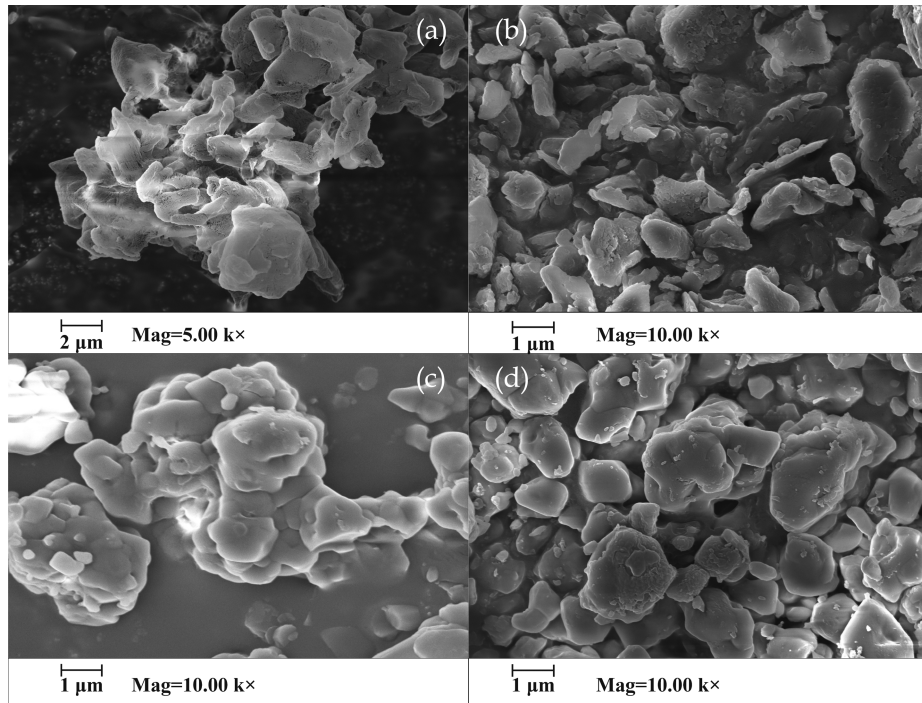


**Figure 3.** SEM images of (a) urea, (b) uracil, and equimolar mixtures of urea and uracil coground for (c) 2 min and (d) 120 min.

absorption spectrum of the powder crystal obtained from equimolar urea and uracil aqueous solution (Figure 1c). In order to obtain a deep insight into the changes of the mixture, external mechanical force was introduced.

The cogrinding process of equimolar stoichiometry of urea and uracil was recorded by THz-TDS system at room temperature. It can be seen from Figure 2a that a new peak showed up at 0.8 THz, and the intensity increased with cogrinding time. It could also be found that the absorption features of the mechanical milling product were the same as that of the product from solution. This demonstrated that uracil and urea can recognize and interact with each other in the solid state.

Figure 2b exhibits the peak intensity at 0.8 THz of the cogrinding mixture as a function of time. The reaction proceeded dramatically before 10 min, then became gentle, and gradually leveled off after 30 min. The result could be explained that upon contact, reactant molecules interacted with each other rapidly but the formed product layer around the reactant particles became a barrier as the reaction proceeded. With the consumption of reactants, the reaction slowed down, but with the help of mechanical grinding, which provided continuous fresh contact between the reacting solids, the reaction would continue smoothly.

Urea has two  $-\text{NH}_2$  groups joined by a carbonyl functional group and is regarded as a good hydrogen bond donor and an excellent receptor. Urea has the ability to trap many organic

compounds. Thus, it is a popular functional molecule for cocrystal design especially in the pharmaceutical industry.<sup>23</sup> Uracil has two carbonyl sites and two amino groups available for hydrogen bonds. Therefore, there is a high possibility for the formation of a cocrystal between urea and uracil with assembly driven through hydrogen bonds. Thus, in this study, we predict that a cocrystal configuration linked by a pair of hydrogen bonds with the structure similar to the pyrimidine base pair in DNA or RNA forms when urea and uracil molecules are put together.

**3.2. SEM.** The surface topography images from the SEM technique gave direct and visual information to help understand the changes during the reaction. Figure 3a,b exhibits the crystal topography of pure urea and uracil, both of which have been pretreated. The particles were flat and thin and had rough, irregular edges. After cogrinding for 2 min, as shown in Figure 3c, uneven clumps with smooth edges started to show up, and some nanoscale particles appeared. After thoroughly grinding for 120 min, a relatively uniform morphology is seen in Figure 3d. The magnification of urea is 5000 times, which is lower than that of uracil and reaction products because of the lower melting point of urea ( $\sim 132$  °C).

Upon grinding, the polycrystalline reactants may experience smash, friction, and collision effects, and the size decreases, and various defects appear, which prompts nucleation and growth of the product crystal.<sup>24</sup> Consequently, the reacting molecules are able to diffuse and migrate in the solid state. The mechanical grinding activates the reaction by overcoming the strong intermolecular force within the crystals and enhances the process kinetics through providing fresh reactive surfaces and mixing the solid reaction mixture.

**3.3. PXRD.** Figure 4 shows a series of PXRD patterns recorded at appropriate times after cogrinding of urea and uracil. The intensity values were normalized. The PXRD patterns of the pure urea and uracil were in good agreement with corresponding PDF cards. The pattern of the initial ( $t = 0$  min) mixture was a combination of peaks of both urea and uracil. However, the situation changed after cogrinding urea and uracil. The peaks corresponding to urea (solid diamonds at  $2\theta = 22.3^\circ$ ,  $24.6^\circ$ , and  $35.5^\circ$ ) and uracil (an open diamond at  $2\theta = 28.3^\circ$ ) decreased with the milling time. Meanwhile, new peaks of the product (open down-pointing triangles at  $2\theta = 11.4^\circ$ ,  $12.7^\circ$ ,  $20.4^\circ$ ,  $23.5^\circ$ ,  $25.6^\circ$ , and  $26.8^\circ$ ) appeared, and the intensities gradually increased when the reaction time was prolonged. The variation trend of the reaction progress was found to be smooth upon exertion of the external mechanical force. From Figure 2c, it was found that the variation trend tracked from THz absorption spectra was quite similar to that in PXRD, that the solid-state reaction was almost completed after 30 min.

The PXRD pattern of the product obtained from 120 min mechanical milling also matched very well with that from the water solution product. This suggests that a cocrystal of urea and uracil was produced efficiently via cogrinding in solid state.

**3.4. Heating Enhanced Reaction.** Heating was also proven to enhance the solid-state reaction in this work. In Figure 5a, the absorption intensity around 0.8 THz increased gradually as temperature increased up to 120 °C. When the temperature was held at 120 °C, the intensity kept rising smoothly at first and then leveled off. Generally, heating activates the reactant molecules and reduces the reaction energy barrier and thus accelerates the reaction as observed in this work. The sample pellet used in this part was made of a

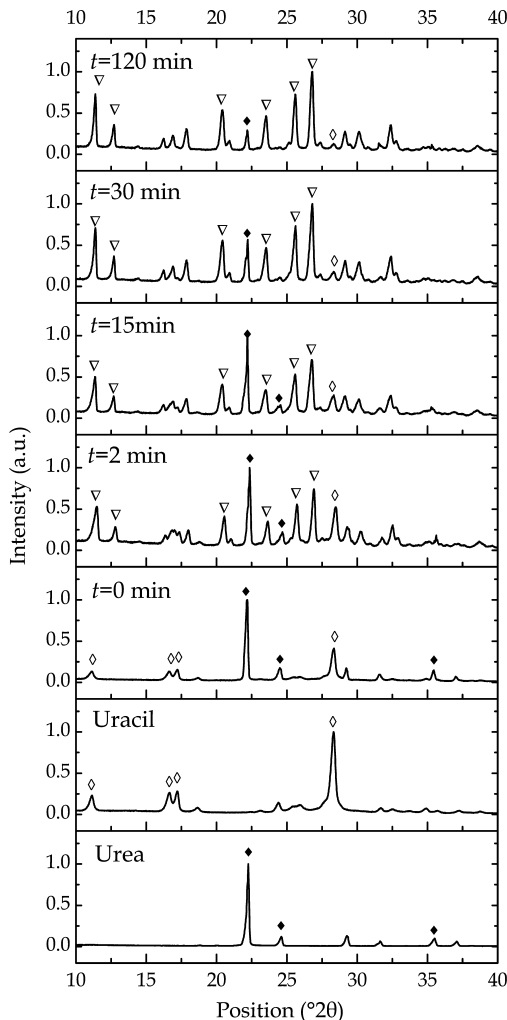


**Figure 4.** PXRD patterns of urea, uracil, and reaction mixtures at different cogrinding periods. Peaks are assigned as those of urea (◆), uracil (◇), and reaction products (▽).

mixture of pretreated reactants (reactants were ground for an hour before the reaction), which lead to the 0.8 THz peak noticeable even at 20 °C. Pretreating reduced the particle size of the reactants. With finer particles, there was greater surface area and more chances to collide and to interact. Thus, the solid-state reaction occurred when the reactants were mixed thoroughly with a pestle and agate mortar.

Figure 5b shows that the absorption peak around 0.8 THz at 20 °C shifts toward lower frequency as the temperature increased. Through the DFT study of uracil–urea dimer in the gas phase, the observed low frequency mode at 0.8 THz was tentatively assigned to a phonon mode within the hydrogen bonded crystal lattice. A weakening of the hydrogen-bond interactions in the vibrational averaged potential at higher temperatures contributes to the red shift of vibration frequency. For low-frequency vibrations, when the temperature rises more molecules are excited to higher energy vibrational states, where the energy level spacing becomes smaller. The decreased energy spacing results in the overall absorption envelope being shifted to lower frequency.<sup>25</sup> In addition, the distribution of the states should be broader at higher temperature, which agrees well with the experimental results that the FWHM of the absorption band broadened as the temperature increased.<sup>26</sup>

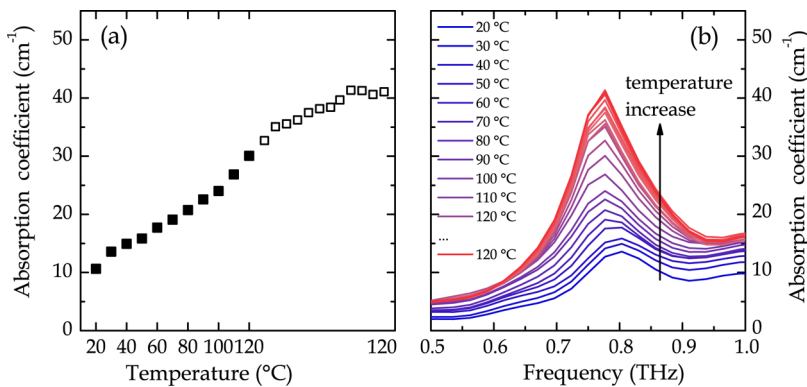


**Figure 5.** (a) THz absorption coefficient of the uracil–urea mixture around 0.8 THz varying with temperature. (b) THz absorption spectrum of the pellet in the frequency range from 0.5 to 1.0 THz recording the heating process from 20 to 120 °C.

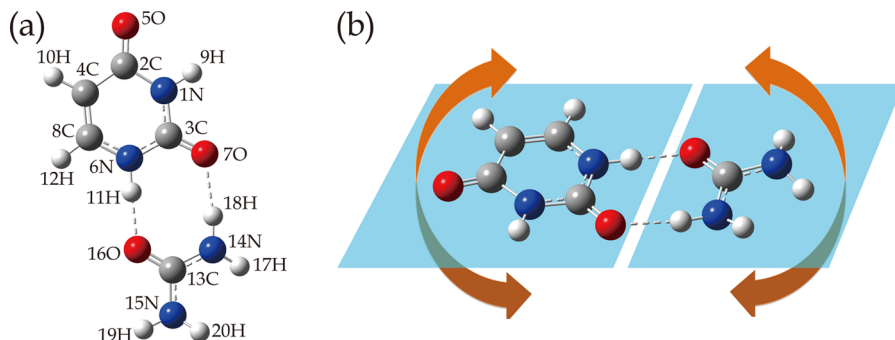


**Figure 6.** (a) Predicted representation of uracil–urea cocrystal structure based on DFT calculations. (b) Calculated vibration mode at 0.94 THz (31.4 cm⁻¹).

**Table 1. Selected FTIR Vibrational Frequencies (cm⁻¹) for Uracil, Urea and Their Heterodimer from the Gas-Phase Calculations, Experimental Data of the Cocrystal, and Tentative Assignments for the Cocrystal**

uracil	calculation			experiment	assignment
	urea	heterodimer	cocrystal <sup>a</sup>		
541	584	600	611 (m)	wagging of C13=O and angle bending of pyrimidine ring	
671		670	716 (vw)	out of plane wagging of N1–H	
767		778	770 (w)	angle bending of pyrimidine ring	
811		813	810 (w)	out of plane wagging of C4/C5–H	
		911	891 (m)	wagging of N–H and C–H	
990	951	997	988 (w)	angle bending of pyrimidine ring and stretching of C13–N	
	1177	1179	1192 (w)	rocking of NH <sub>2</sub> of N14 and N15 and stretching of C13=O	
1189		1203	1227 (sh)	stretching of pyrimidine ring	
1226		1253	1242 (sh)		
	1632	1629	1649 (sh)	scissoring of NH <sub>2</sub> of N14/N15 and stretching of C13=O	
		1652	1676 (sh)		
		1733	1776 (vw)		
1768	1787	1733	1720 (vs)	stretching of C=O	
1803		1757	1776 (w)		
		1775	1790 (w)		
3637		3155	3227 (m)	stretching of N3–H	
	3690	3398	3331 (w)	asymmetric stretching of NH <sub>2</sub> of N14	
	3580	3589	3429 (m)	symmetric stretching of NH <sub>2</sub> of N15	

<sup>a</sup>Abbreviations used: vw, very weak; w, weak; m, medium; s, strong; vs, very strong; sh, shoulder.

**3.5. DFT Calculation and Analyses.** To rationalize the observed transformation in the experiment, the cocrystallization manner was investigated using DFT calculations. The B3LYP exchange-correlation functional<sup>27</sup> within the generalized gradient approximation (GGA) in the framework of DFT was used in the DFT-based calculations. Three- $\zeta$  basis 6-311+

+G(d,p) was employed with a polarization and diffuse function added on every atom. All calculations were conducted using the Gaussian-09 package.<sup>28</sup>

Figure 6 shows the representation of uracil–urea cocrystal structure after the geometry optimization. It is a planar hydrogen bonding configuration similar to the hydrogen

bonding pattern between nucleobases observed in native DNA or RNA molecules. Uracil has alternating proton donor and acceptor sites,<sup>29</sup> so three different positions exist for possible hydrogen-bonding interaction. The one shown in Figure 6a is the most preferred site with the largest interaction energy and the best agreement with experiment. The binding energy,  $E_{\text{binding}} = -0.6885 \text{ eV}$ , was calculated via the following equation,

$$E_{\text{binding}} = E_{\text{cocrystal}} - (E_{\text{uracil}} + E_{\text{urea}}) \quad (1)$$

The vibrational frequencies were calculated based on the optimized structure and were tentatively assigned to the observed THz features. One vibration mode is found at 0.94 THz ( $31.4 \text{ cm}^{-1}$ ), which corresponds to butterfly motion between urea and uracil through a pair of hydrogen bonds, shown in Figure 6b. This mode can be well assigned to the prominent absorption peak at 0.8 THz ( $26.7 \text{ cm}^{-1}$ ) in the experiment. A second one locates at 1.70 THz ( $56.8 \text{ cm}^{-1}$ ), corresponding to the hindered rotations of uracil and urea molecules, can be assigned to the experimental 1.6 THz ( $53.3 \text{ cm}^{-1}$ ) absorption peak.

A specific feature of H-bonded dimers or heterodimers is the strong coupling of the NH/OH stretching vibrations with some low-frequency intermolecular modes.<sup>30–32</sup> In a solid, rocking or stretching intermolecular modes are sufficiently strongly coupled with the proton motion.<sup>33,34</sup>

In addition, the experimental FTIR spectra were also assigned according to the calculated modes. The obtained FTIR spectra revealed the vibrational mode information on the tested compounds and can be used for characterizing and identifying different solid-state forms. Selected FTIR vibrational frequencies ( $\text{cm}^{-1}$ ) for uracil, urea, and their heterodimer from the gas-phase calculations, the experimental data from the cocrystal, and tentative assignments for the cocrystal are given in Table 1. The spectrum of the cocrystal has similar characteristic bands as that of uracil and urea but with different levels of frequency shifts originating from the interaction and the circumstance change of the moieties: for instance, in the uracil moiety, the angle bending of the pyrimidine ring at  $778 \text{ cm}^{-1}$  and the stretching of the pyrimidine ring at 1203 and  $1253 \text{ cm}^{-1}$ , and in the urea moiety, the overlapped NH<sub>2</sub> rocking and C=O stretching at  $1179 \text{ cm}^{-1}$ . All of them significantly shift from the original vibration frequency in the moieties. Likewise, in the  $3000\text{--}3700 \text{ cm}^{-1}$  region, the cocrystal vibrational frequencies of the stretching of N3-H and NH<sub>2</sub> of N14/N15 distinguish remarkably from the reactants. Furthermore, several bands of the reactant still remain in the cocrystal. For instance, the out-of-plane wags of N-H and C-H at 670 and  $813 \text{ cm}^{-1}$  in the uracil moiety of the cocrystal vary little from uracil. Some vibrational bands result from the collaborative vibration of both moieties lead by the hydrogen bonds between O7-H18 and O16-H11 and thus deviate much from the corresponding bands of uracil and urea, for example, C13=O wagging and pyrimidine ring angle bending at  $600 \text{ cm}^{-1}$ , C13-N stretching and pyrimidine ring angle bending at  $997 \text{ cm}^{-1}$ , and C=O group stretching at 1733, 1757,  $1775 \text{ cm}^{-1}$ , all of which accompany the stretches and deformations of the hydrogen bonds. The overall discrepancy of the vibrational frequencies between the calculation and the experiment can be ascribed to the interaction with the surrounding molecules, the temperature influences, and the vibrational anharmonicity.

## 4. CONCLUSION

We proved that a cocrystal of urea and uracil formed via solid-state reaction in dry environment, and the process was monitored by THz-TDS. Mechanical grinding and increasing temperature were proven to be able to enhance the solid-state reaction. The experimental results indicate that the recognition and interaction can take place with high efficient between urea and uracil without water molecule participation. The results of THz spectroscopy agreed with the PXRD and FTIR measurements very well. DFT theoretical calculation was performed, and the absorption features in THz and FTIR spectra were tentatively assigned. The calculations agreed with the experimental observation. The results indicated that uracil and urea crystallize in planar hydrogen-bonded uracil–urea pairs, which is similar to the manner found in DNA or RNA. Comparison between the approaches we employed in this study revealed that THz spectroscopy is extremely sensitive to the hydrogen bonding interaction and is proven to be simpler and more convenient in quantitative analysis and online monitoring owing to a directly characteristic feature in the far-infrared region.

## ■ ASSOCIATED CONTENT

### S Supporting Information

Complete references 17 and 28. This material is available free of charge via the Internet at <http://pubs.acs.org>.

## ■ AUTHOR INFORMATION

### Corresponding Authors

\*Tel.: +86-21-39194818. Fax: +86-21-39194818. E-mail address: zhaohongwei@sinap.ac.cn. Mailing address: Jiading campus, 2019 Jia Luo Road, Jiading District, Shanghai 201800, P. R. China.

\*Tel.: +86-22-27891103. Fax: +86-22-27891103. E-mail address: jiaghan@tju.edu.cn. Mailing address: 92 Weijin Road, Nankai District, Tianjin 300072, P. R. China.

### Notes

The authors declare no competing financial interest.

## ■ ACKNOWLEDGMENTS

The research was supported by National Science Foundation of China (Grant Nos. 10574134 and 10675157) and National Basic Research Program of China (Grant Nos. 2014CB3398, 2010CB832903, and Y329021011).

## ■ REFERENCES

- (1) Bolivar, P. H.; Brucherseifer, M.; Nagel, M.; Kurz, H.; Bosserhoff, A.; Buttner, R. Label-Free Probing of Genes by Time-Domain Terahertz Sensing. *Phys. Med. Biol.* **2002**, *47*, 3815–3821.
- (2) Fischer, B. M.; Walther, M.; Uhd Jepsen, P. Far-Infrared Vibrational Modes of DNA Components Studied by Terahertz Time-Domain Spectroscopy. *Phys. Med. Biol.* **2002**, *47*, 3807–3814.
- (3) Nishizawa, J.; Sasaki, T.; Suto, K.; Tanabe, T.; Saito, K.; Yamada, T.; Kimura, T. THz Transmittance Measurements of Nucleobases and Related Molecules in the 0.4-to 5.8-THz Region Using a GaP THz Wave Generator. *Opt. Commun.* **2005**, *246*, 229–239.
- (4) Brucherseifer, M.; Nagel, M.; Bolivar, P. H.; Kurz, H.; Bosserhoff, A.; Buttner, R. Label-free Probing of the Binding State of DNA by Time-Domain Terahertz Sensing. *Appl. Phys. Lett.* **2000**, *77*, 4049–4051.
- (5) Li, X.; Globus, T.; Gelmont, B.; Salay, L. C.; Bykhovski, A. Terahertz Absorption of DNA Decamer Duplex. *J. Phys. Chem. A* **2008**, *112*, 12090–12096.

- (6) Wu, X. J.; E, Y. W.; Xu, X. L.; Wang, L. Label-Free Monitoring of Interaction Between DNA and Oxaliplatin in Aqueous Solution by Terahertz Spectroscopy. *Appl. Phys. Lett.* **2012**, *101*, 033704.
- (7) Arora, A.; Luong, T. Q.; Kruger, M.; Kim, Y. J.; Nam, C.-H.; Manz, A.; Havenith, M. Terahertz Time-Domain Spectroscopy for the Detection of PCR Amplified DNA in Aqueous Solution. *Analyst* **2012**, *137*, 575–579.
- (8) Dallmann, A.; Pfaffe, M.; Mügge, C.; Mahrwald, R.; Kovalenko, S. A.; Ernsting, N. P. Local THz Time Domain Spectroscopy of Duplex DNA via Fluorescence of an Embedded Probe. *J. Phys. Chem. B* **2009**, *113*, 15619–15628.
- (9) King, M. D.; Ouellette, W.; Korter, T. M. Noncovalent Interactions in Paired DNA Nucleobases Investigated by Terahertz Spectroscopy and Solid-State Density Functional Theory. *J. Phys. Chem. A* **2011**, *115*, 9467–9478.
- (10) King, M. D.; Korter, T. M. Noncovalent Interactions between Modified Cytosine and Guanine DNA Base Pair Mimics Investigated by Terahertz Spectroscopy and Solid-State Density Functional Theory. *J. Phys. Chem. A* **2011**, *115*, 14391–14396.
- (11) Nguyen, K. L.; Friscic, T.; Day, G. M.; Gladden, L. F.; Jones, W. Terahertz Time-Domain Spectroscopy and the Quantitative Monitoring of Mechanochemical Cocrystal Formation. *Nat. Mater.* **2007**, *6*, 206–209.
- (12) Parrott, E. P. J.; Zeitler, J. A.; Friscic, T.; Pepper, M.; Jones, W.; Day, G. M.; Gladden, L. F. Testing the Sensitivity of Terahertz Spectroscopy to Changes in Molecular and Supramolecular Structure: A Study of Structurally Similar Cocrystals. *Cryst. Growth Des.* **2009**, *9*, 1452–1460.
- (13) Charron, D. M.; Ajito, K.; Kim, J. Y.; Ueno, Y. Chemical Mapping of Pharmaceutical Cocrystals Using Terahertz Spectroscopic Imaging. *Anal. Chem.* **2013**, *85*, 1980–1984.
- (14) Mehra, R.; Yadav, P. Acoustic and Volumetric Studies of Uracil in Aqueous Urea Solution at Different Temperatures. *Phys. Chem. Liq.* **2012**, *50*, 88–101.
- (15) Srivastava, T.; Pandey, A.; Sethi, R.; Haroon, S.; Pandey, J. D.; Misra, K. Interaction of Uracil and Uridine with the Cosolvent and Denaturant Aqueous Urea at Molecular Level: Effect of  $\text{Na}^+$ ,  $\text{K}^+$  and  $\text{Ca}^{++}$  Ions. *Proc. Natl. Acad. Sci., India, Sect. A* **2012**, *82*, 179–186.
- (16) Hong, J.; Capp, M. W.; Anderson, C. F.; Saecker, R. M.; Felitsky, D. J.; Anderson, M. W.; Record, M. T. Preferential Interactions of Glycine Betaine and of Urea with DNA: Implications for DNA Hydration and for Effects of These Solutes on DNA Stability. *Biochemistry* **2004**, *43*, 14744–14758.
- (17) Guinn, E. J.; Schwinefus, J. J.; Cha, H. K.; McDevitt, J. L.; Merker, W. E.; Ritzer, R.; Muth, G. W.; Engelsgjerd, S. W.; Mangold, K. E.; Thompson, P. J.; et al. Quantifying Functional Group Interactions that Determine Urea Effects on Nucleic Acid Helix Formation. *J. Am. Chem. Soc.* **2013**, *135*, 5828–5838.
- (18) Yoon, J.; Thirumalai, D.; Hyeon, C. Urea-Induced Denaturation of PreQ(1)-Riboswitch. *J. Am. Chem. Soc.* **2013**, *135*, 12112–12121.
- (19) Funkner, S.; Havenith, M.; Schwaab, G. Urea, a Structure Breaker? Answers from THz Absorption Spectroscopy. *J. Phys. Chem. B* **2012**, *116*, 13374–13380.
- (20) Yang, Z.; Xiu, P.; Shi, B.; Hua, L.; Zhou, R. Coherent Microscopic Picture for Urea-Induced Denaturation of Proteins. *J. Phys. Chem. B* **2012**, *116*, 8856–8862.
- (21) Grischkowsky, D.; Keiding, S.; Vanexter, M.; Fattinger, C. Far-Infrared Time-Domain Spectroscopy with Terahertz Beams Of Dielectrics and Semiconductors. *J. Opt. Soc. Am. B* **1990**, *7*, 2006–2015.
- (22) Han, J.; Zhang, W.; Chen, W.; Thamizhmani, L.; Azad, A. K.; Zhu, Z. Far-Infrared Characteristics of ZnS Nanoparticles Measured by Terahertz Time-Domain Spectroscopy. *J. Phys. Chem. B* **2006**, *110*, 1989–1993.
- (23) Onija, O.; Borodi, G.; Kacsó, I.; Pop, M. N.; Dadarlat, D.; Bratu, I.; Jumate, N. Preparation and Characterization of Urea-Oxalic Acid Solid Form. *AIP Conf. Proc.* **2012**, *1425*, 35–38.
- (24) Ge, M.; Wang, W. F.; Zhao, H. W.; Zhang, Z. Y.; Yu, X. H.; Li, W. X. Characterization of Crystal Transformation in the Solid-State by Terahertz Time-Domain Spectroscopy. *Chem. Phys. Lett.* **2007**, *444*, 355–358.
- (25) Shen, Y. C.; Upadhyay, P. C.; Linfield, E. H.; Davies, A. G. Temperature-Dependent Low-frequency Vibrational Spectra of Purine and Adenine. *Appl. Phys. Lett.* **2003**, *82*, 2350–2352.
- (26) Hoshina, H.; Morisawa, Y.; Sato, H.; Minamide, H.; Noda, I.; Ozaki, Y.; Otani, C. Polarization and Temperature Dependent Spectra of Poly(3-hydroxyalkanoate)s Measured at Terahertz Frequencies. *Phys. Chem. Chem. Phys.* **2011**, *13*, 9173–9179.
- (27) Lee, C. T.; Yang, W. T.; Parr, R. G. Development of the Colle-Salvetti Correlation-Energy Formula into a Functional of the Electron-Density. *Phys. Rev. B* **1988**, *37*, 785–789.
- (28) Frisch, M. J.; Trucks, G. W.; Schlegel, H. B.; Scuseria, G. E.; Robb, M. A.; Cheeseman, J. R.; Scalmani, G.; Barone, V.; Mennucci, B.; Petersson, et al. *Gaussian 09*, Revision A.01; Gaussian, Inc.: Wallingford, CT, 2009.
- (29) Hunter, K. C.; Rutledge, L. R.; Wetmore, S. D. The Hydrogen Bonding Properties of Cytosine: A Computational Study of Cytosine Complexed with Hydrogen Fluoride, Water, and Ammonia. *J. Phys. Chem. A* **2005**, *109*, 9554–9562.
- (30) Fuke, K.; Kaya, K. Dynamics of Double-Proton-Transfer Reaction in the Excited-State Model Hydrogen-Bonded Base-Pairs. *J. Phys. Chem.* **1989**, *93*, 614–621.
- (31) Sekiya, H.; Nagashima, Y.; Nishimura, Y. Electronic-Spectra of Jet-Cooled Tropolone - Effect of the Vibrational-Excitation on the Proton Tunneling Dynamics. *J. Chem. Phys.* **1990**, *92*, 5761–5769.
- (32) Douhal, A.; Lahmani, F.; Zewail, A. H. Proton-Transfer Reaction Dynamics. *Chem. Phys.* **1996**, *207*, 477–498.
- (33) Meyer, R.; Ernst, R. R. Transitions Induced in a Double Minimum System by Interaction with a Quantum-Mechanical Heat Bath. *J. Chem. Phys.* **1990**, *93*, 5518–5532.
- (34) Sakun, V. P.; Vener, M. V.; Sokolov, N. D. Proton Tunneling Assisted by the Intermolecular Vibration Excitation. Temperature Dependence of the Proton Spin-Lattice Relaxation Time in Benzoic Acid Powder. *J. Chem. Phys.* **1996**, *105*, 379–387.